Environmental Technology & Science Journal
Vol. 12 Number 2 December 2021

# Comparative Assessment of SRTM and UAV-Derived Dem in Flood Modelling

**Adesina E. A, Musa A, Ajayi O. G, Odumosu J. O, Opaluwa Y. D & Onuigbo I. C**
Department of Surveying & Geoinformatics, Federal University of Technology, Minna
Correspondence: geoworldsolutions007@gmail.com

**Received: 14/01/2022** **Revised: 27/01/2021** **Accepted: 10/02/2022**

Flooding is one of the most devastating natural disasters occurring annually in many parts of the world. This study investigates the performance of DEM with different spatial resolution in flood modelling along the floodplain of Shiroro dam, Nigeria. Three different DEMs of 30 m, 15 m and 3 m spatial resolution covering the study area were investigated. The performance of the DEMs for flood modelling was evaluated with the aid of flood inundation modelling (3D analyst) tools in the ArcScene environment of ArcGIS 10.4 using results obtained from the shallow water St. Venant's equation. The shallow water St. Venant's equation was implemented in MATLAB software using the given river bathymetric information obtained from the dam authorities. The study determined the discharge quantity and flow velocity at some identified nodes along the river and its tributaries, thus, providing a basis for determining possible flood levels within the study area. Three flood levels were identified for each of the three used DEMs. For the original and re-sampled SRTM DEMs, the identified flood levels were 200 m, 250 m and 280 m, while for the UAV-derived DEM, 150 m, 205 m and 250 m were identified as the flood levels. Flood events covering the three identified flood levels were then simulated in ArcScene in order to estimate inundating settlements within the study area. The original 30 m and 15 m resampled resolution SRTM DEM had maximum and minimum height values of 612 m, 125 m and 585 m, 136 m respectively. In contrast, the UAV-derived DEM shows different characteristics, with maximum and minimum values of 497.22 m and 113.53 m, respectively. Further analysis showed that while the UAV derived DEM reliably predicted the flood risk situation due to its high resolution, the other two DEMs over predicted the flood risk situation of the area.

**Keywords:** DEM resolution, Floodplain modelling, Shiroro dam, UAV and Vulnerability
**DOI:** https://dx.doi.org/10.4314/etsj.v12i2.6

## INTRODUCTION

Societal needs for reliable information on flood characteristics are increasing as the occurrence of flood events has become a common experience in many parts of the world due to global warming and increase in rainfall, coupled with anthropogenic activities which include construction of houses along the floodplains (Usman and Ifabiyi, 2012; Pena and Nardi, 2018). Depending on the magnitude of the flood, the occurrence often results in loss of lives and property with huge economic implications. More than two billion peoples who lived in floodplains worldwide between 1998 and 2017 were affected by flood disaster (WHO, 2020). It was also estimated that Nigeria suffered combined losses of more than $16.9 billion in damaged properties, oil production, agricultural and other losses due to flood events in 2012 alone (Komolafe, 2015; Egbenta *et al.*, 2015).

Environment Agency (EA) opined that there are 2.7 million properties at risk of fluvial and coastal flooding, three million properties at risk of pluvial flooding and 660,000 at risk from both (Environment

Agency, 2018). Furthermore, with an amorphous population growth, construction and development of dwellings on floodplains (Pottier *et al.,* 2005) and more extreme and intense rainfall events due to phenomenon such as global warming (Ward *et al.,* 2014; Corringham and Cayan, 2019), the frequency, magnitude and impacts of flood events are only going to increase, which makes accurate modelling, prediction and forecasting of future flooding occurrences highly important as it will ensure better management of flood risks.

The rapid advancement in remote sensing data collection and monitoring over the last decade has facilitated more widespread flood modelling activities (Keshtkar *et al.,* 2017). The wide availability of Digital Elevation Models (DEM) together with supercomputers to handle the required simulation power has made 2D flood modelling the preferred option for predicting flood properties including extent, depth and velocity, especially in urban areas where surface dynamics are very high. The equations governing the hydrodynamic behaviour of an incompressible fluid are based on the classical concepts of conservation of mass and momentum. For many practical surface-water flow applications, knowledge of the full three-dimensional flow structure is not required, and it is sufficient to use mean- flow quantities in two perpendicular horizontal directions (Laxmi and Narendra, 2016). 2D flood models have the capability to model the flow in both directions i.e. along the river and perpendicular to the river (Tarekegn *et al.*, 2010). The 2D flood model main inputs are river and floodplain geometric data, hydraulic parameters and boundary conditions. With the extensive use of 2D flood models, the resolution and quality of DEMs have come under greater focus especially in urban hydrology (Ozdemir *et al.,* 2013; Saksena and Merwade, 2015; Pena and Nardi, 2018; Ogania *et al.,* 2019).

Nevertheless, researchers have continued to study the effect of DEM resolution on the estimation of flood properties (Balica *et al.,* 2012; Aerts *et al.,* 2014; Barraga´n *et al.,* 2015; Zazo *et al.,* 2015; Jafarzadegan and Merwade, 2017; Hawker *et al.,* 2018; Bhuyian and Kalyanapu, 2018; Nkwunonwo *et al.,* 2019; Lim and Brandt, 2019; Karamuz *et al.,* 2020; Kepeng *et al.,* 2021; Talchabhadel *et al.,* 2021). While some of these efforts opined that higher resolution DEMs produce more accurate flood modelling, Azizian and Brocca, (2020) affirmed that it is not necessarily the highest resolution DEM, but the optimal resolution DEM, that produces most reliable flood modelling result.

Saksena and Merwade (2015) analysed a range of DEM resolutions from 6 m to 30 m in flood modelling and sought to relate the differences arising from the use of the various DEM resolutions with the resultant flood inundation maps and then use this information to create improved flood inundation maps from low-resolution DEMs. It was observed that increasing the grid size of the DEM increased the flood areas and flood depths. However, regardless of flood type, low-resolution DEMs will always result in an overprediction of flood extent and depth. In contrast, other studies have shown the opposite trend for surface water flooding (Mukherjee *et al.,* 2013; Hawker *et al.,* 2018; Ogania *et al.,* 2019; Mohamed and Ali, 2019; Talchabhadel *et al.,* 2021; Kepeng *et al.,* 2021).

To this end, the aim of this study is to investigate how DEM resolution affects flood modelling results along the floodplains of Shiroro dam, Nigeria. Three DEMs of different resolution, covering the study area were investigated. These DEMs are: (i) 1 arcsec Shuttle Radar Topographic Mission (SRTM) DEM (i.e. 30 m spatial resolution), (ii) resampled SRTM DEM re-sampled of 15 m spatial resolution and (iii) 3 m resolution DEM generated from a UAV mission. The performance of the 3 DEMs for flood modelling was evaluated with the aid of flood inundation modelling tools in the Arc Scene environment of ArcGIS 10.4 using shallow water St. Venant’s equation.

## MATERIAL AND METHODS

### Study Site

The study area is Shiroro dam floodplain, located in Shiroro Local Government Area of Niger State, Nigeria. It is situated between Longitude 6º 27’ 00’’E to 7º 05’ 30’’E and Latitude 09º 44’ 00’’N to 10º 11’ 30’’N. It is 550.364 meters downstream of the confluence of River Kaduna and River Dinya at Shiroro village. There are tributaries of the River Kaduna within the Shiroro watershed, chief among them being rivers Dinya, Sarkin Pawa, Guni, Erena and Muyi. The tributaries flow majorly in the north-south direction while the remaining tributaries flow in the northwest to southeast direction. The area is generally low lying with some conspicuous hills and it is well drained by River Shiroro and its tributaries (Adie *et al*., 2012). The land use activities within the area include residential and agricultural. The dam is used basically for hydroelectric power generation. Due to high elevation difference, the risk of damage caused by flood is very high in this area. The general climate of the study area is the Tropical Monsoon type characterized by alternate wet and dry season, with rainfall occurring in the rainy seasons of May to October. Temperatures are relatively high throughout the year hovering between 27$^0$C and 35$^0$C (Suleiman, 2014). Rain starts in April and the length of raining season is between 161-200 days (Anzaku *et al.*, 2019).

Flood occurrence within the study area has become an annual occurrence which peaks at raining season. Specifically, in recent years, different flood scenarios of varying magnitude of consequential effect have been experienced in 1990,1992, 1994, 1996, 1998, 1999 to 2000, 2003, 2006, 2010, 2012, 2015, 2018, 2019 and 2020 (NEMA, 2020). The major causative factor of this flood is the opening of the dam’s spillways (Usman and Ifabiyi, 2012; Abayomi *et al.*, 2015) to the downstream of the study area in a bid to reduce the water volume when it exceeds the dam’s capacity to avoid dam collapse or failure. Figure 1 shows the map of the study area while Figure 2 depicts Shiroro dam and the downstream flow of water.

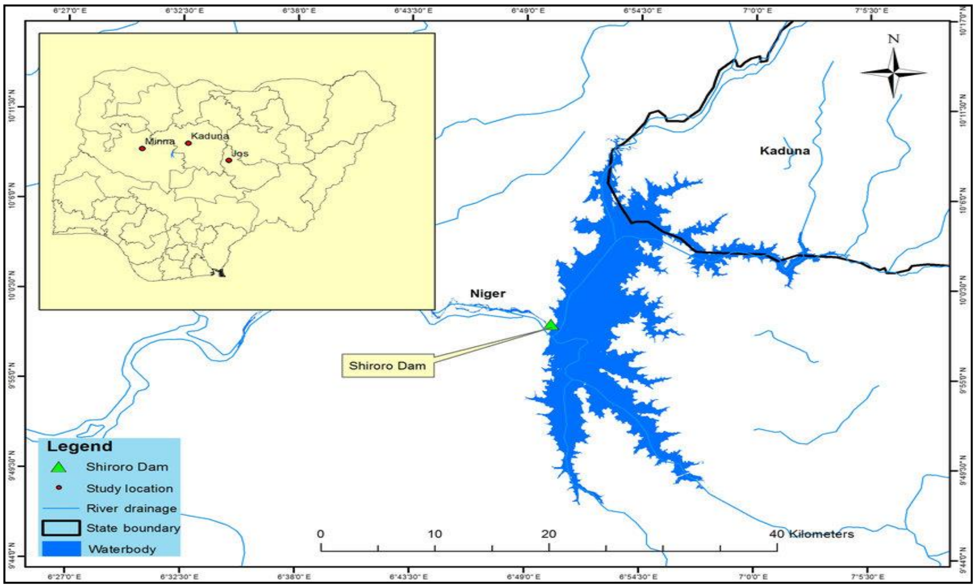


**Figure 1: Map of the study area**
**Source: Ministry of land and survey, Minna, Niger State**

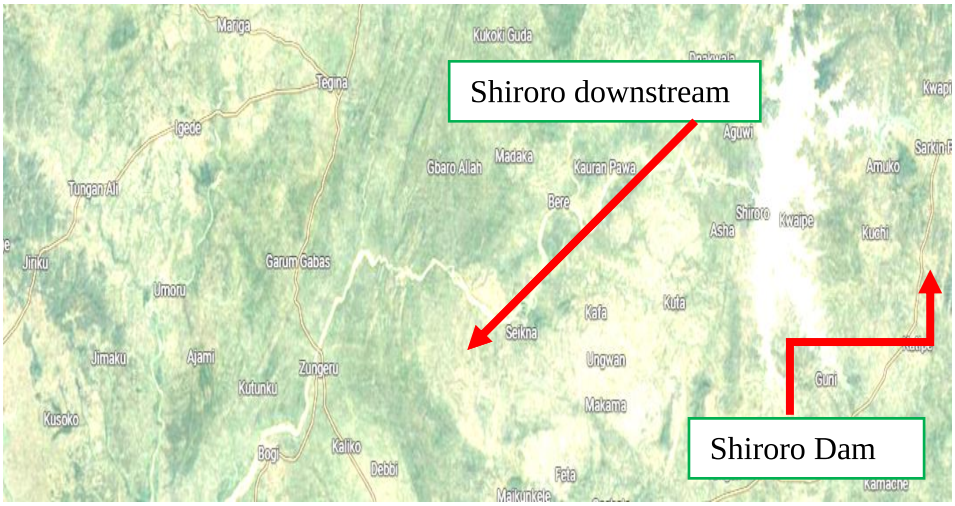


**Figure 2: Shiroro dam and the downstream flow of water (Source: Google Earth Map)**

## Data Acquisition

The data type, source and characteristics of data used for this study are presented in Table 1.

**Table 1: Details of the data used for the study**

| S/N | Data | Source | Spatial resolution | Date of data acquisition | Accuracy |
|---|---|---|---|---|---|
| i | SRTM 30 m DEM | (USGS, http://earthexplorer.usgs.gov) | 30 m | 2000 | 3-4 m |
| ii | SRTM 15m DEM | Resampled from SRTM of 30 m DEM | 15 m | 2000 | 5 m |
| iii | UAV - derived DEM | Field mission | 3 m | 2019 | 1.5 m |
| iv | River channel Bathymetry | Dam authority | - | 2020 | - |
| v | Water discharge | Dam authority | - | 2020 | - |
| vi | Water level | Dam authority | - | 2020 | - |

A Trimble UX5 aerial imaging solution was deployed for the acquisition of the UAV images of the study area. The acquired images were processed using Trimble Business Center Photogrammetry Module (Version 3.30). The data was post-processed in UTM 32N projected coordinate system referenced to the WGS84 global ellipsoid. 52 GCPs were established across the study area and only 20GCPs were used for the adjustment of tie points (aero-triangulation) succeeded by the production of Digital Elevation Model. Details of the flight parameters for the UAV mission are as provided in Table 2. The processing software (Trimble Business Center Photogrammetry Module (Version 3.30)) was also used to extract the height of the buildings from the digital surface model in order to achieve the digital elevation model for the study area which is the major concern of this research.

**Table 2: Flight planning parameters for the UAV mission**

| S/N | Parameter | Value |
|---|---|---|
| i | Flying height | 200 m |
| ii | Flight speed | 8-15 m/s |
| iii | Forward lap | 65% |
| iv | Side lap | 70% |
| v | focal length | 24mm |
| vi | Flight time is approximately | 15minutes |
| vii | Battery capacity | 25-30minutes |
| viii | Flight time | 15minutes |
| ix | Number of GCPs | 52points |
| x | Number of GCPs used for georeferenced | 32points |
| xi | Number of GCPs used for the adjustment of Tie points | 20points |

**The DEMs**

The statistics of the three different DEMs of different spatial resolutions used in this study are presented in Table 3 while Figures 3(a - c) show the 30 m SRTM DEM, the 15 m re-sampled SRTM DEM and the 3 m UAV-derived DEM.

**Table 3: Statistics of the 3 DEM's**

| Parameter | SRTM 30m resolution | 15m re-sampled SRTM DEM | 3m UAV-derived DEM |
|---|---|---|---|
| Min height | 125 | 136 | 113.53 |
| Max height | 612 | 585 | 497.22 |
| Range | 487 | 449 | 389.69 |
| Standard Deviation | 68.38 | 67.58 | 63.16 |

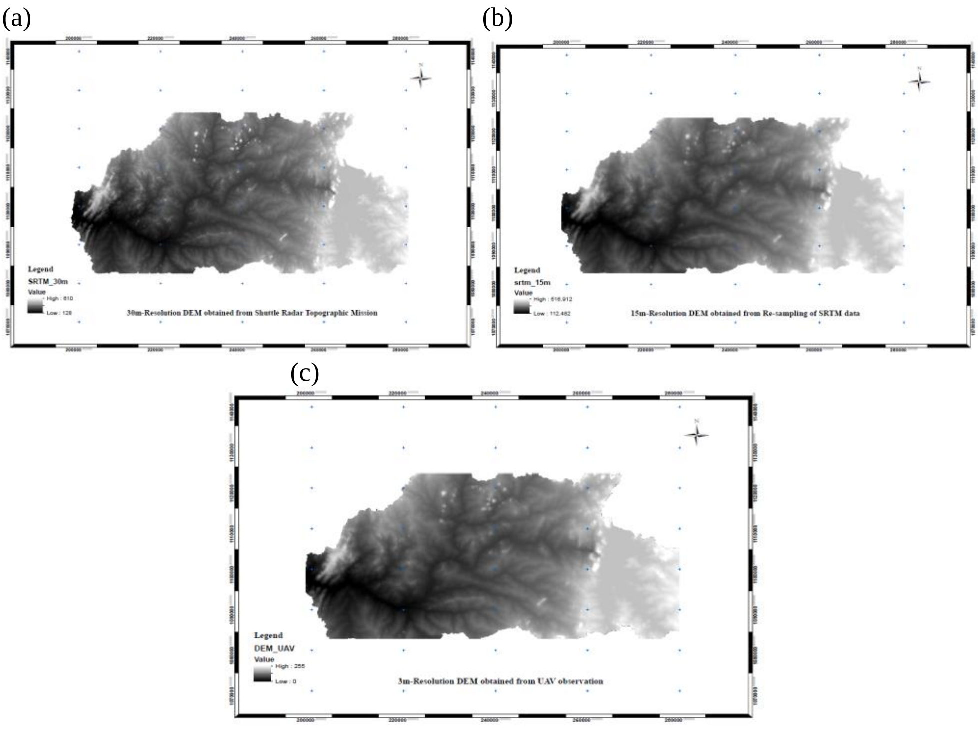


**Figure 3: (a) 30 m DEM (b) 15 m-Resampled DEM (c) 3 m UAV-derived DEM**

**Flood Simulation Approach**

The 2D flood inundation modelling was carried out using ArcGIS 10.4. ArcScene in ArcGIS 10.4 is capable of simulating surface flooding caused by rainfall as well as river flooding. Prior to flood simulation in ArcScene, the river discharge and flow velocity were computed in MATLAB software using the conventional shallow water St. Venant's equation as given by (Brunner *et. al.,* 2020) (see Equations 1):

$$\frac{\partial Q}{\partial t} + \frac{\partial}{\partial x}\left(\frac{Q^2}{A}\right) = -gAS_f + gAS_o - gA\frac{\partial h_o}{\partial x} \quad (1)$$

*where,*

$Q$ = discharge

$A$ = cross-sectional area

$\frac{\partial Q}{\partial t}$ = rate of discharge with respect to time

$\frac{\partial}{\partial x}\left(\frac{Q^2}{A}\right)$ = rate of discharge with respect to cross-sectional area

$g$ = acceleration due to gravity

$S_f$ = frictional slope

$S_o$ = reference slope

$\frac{\partial h_o}{\partial x}$ = channel bed-topography; where $Q$ can be computed as:

$$Q = \frac{A}{n} * R^{\frac{2}{3}} * S^{\frac{1}{2}} \quad (2)$$

*where,*

$R$ =hydraulic radius

$n$ =Manning coefficient of roughness

$A$ = cross-sectional area

$S$ = channel slope in the direction of flow

$\frac{\partial h_o}{\partial x}$ is obtained from the Digital Elevation Model (DEM),

$A$ is measured on ground and

$S_f$ and $S_o$ deduced from $\frac{\partial h_o}{\partial x}$

$Q$ is computed using equation (2)

Thus, by simultaneous substituting the computed value of $Q$ and $A$ from equation (2) into equation (1) allow us to calculate the actual flow rate $\frac{\partial Q}{\partial t}$ in Equation (1).

## RESULTS AND DISCUSSION

Figures 3a to 3c presents the DEMs used for this research. The closeness in value of standard deviation between SRTM of 30m resolution and 15m re-sampled SRTM DEM further show that both the datasets are of the same source and have similar level of accuracy and spatial attributes.

**Derived Flood-levels**

The three DEMs were tested to determine flood levels capable of inundating the studied floodplains. Figure 4 shows the delineated catchment area and drainage basin from all the three (30 m, 15 m, and 3 m) resolution DEMs. The size of the drainage basin is about 2000sq.km and the catchment area is about 466.995sq.km, a total of about 12 water channels were identified to be contributing significantly to the flow of water within catchment area (Figure 4), signifying that the stream flows frequently downstream with a gentle slope or gradient.

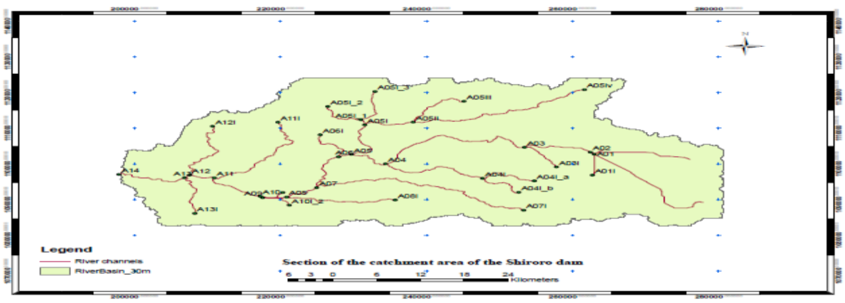


**Figure 4: Delineated catchment area from the 30 m, 15 m and 3 m resolution DEMs**

To compute the flood levels, equations 1 to 2 were implemented in the MATLAB software using the given river bathymetry and the three different DEMs. Using the starting and ending nodes as major identification points along the 12 identified water channels (catchment areas) for the stream, the river discharge of each of the identified nodes provided a basis for the determination of levels that can be obtained from the stream given an initial discharge of $114.38m/s^3$. The used initial discharge value corresponds to the dam discharge when the spillway is opened (Dam Authorities, 2020). Table 4 shows the computed discharge and flow velocity at each of the nodes.

**Table 4: Discharge rate at selected nodes within the Shiroro dam basin using 30 m, 15 m and 3 m DEMs**

| | | 30 m DEM | | | 15 m DEM | | | 3 m DEM | | |
|---|---|---|---|---|---|---|---|---|---|---|
| Sta_ID | Settlements Name | Elevation (m) | Discharge (m/s^3) | Velocity (m/s^2) | Elevation (m) | Discharge (m/s^3) | Velocity (m/s^2) | Elevation (m) | Discharge (m/s^3) | Velocity (m/s^2) |
| A01 | Gidan Patuko | 373.07 | 114.38 | 1.27 | 373.08 | 114.38 | 1.27 | 345.61 | 114.38 | 1.27 |
| A02 | Gidan Patuko | 280.09 | 1154.42 | 9.07 | 280.21 | 1153.72 | 9.06 | 304.23 | 770.10 | 6.05 |
| A03 | Awolu Saga | 256.09 | 219.00 | 1.53 | 256.95 | 215.59 | 1.51 | 228.89 | 387.96 | 2.72 |
| A04 | Sumaila | 223.20 | 152.48 | 1.12 | 223.20 | 154.47 | 1.13 | 194.86 | 155.12 | 1.13 |
| A05 | Bere | 211.10 | 293.92 | 1.35 | 211.07 | 294.28 | 1.35 | 183.78 | 281.24 | 1.29 |
| A06 | Tungan Gamba | 209.33 | 146.16 | 0.94 | 209.32 | 144.95 | 0.93 | 184.77 | 108.94 | 0.70 |
| A07 | Layi | 197.05 | 227.45 | 1.06 | 196.13 | 235.77 | 1.09 | 168.08 | 265.17 | 1.23 |
| A08 | Nil | 174.97 | 314.13 | 1.99 | 174.98 | 307.48 | 1.95 | 147.31 | 304.65 | 1.93 |
| A09 | Nil | 174.39 | 69.90 | 0.43 | 174.40 | 69.91 | 0.43 | 144.60 | 151.13 | 0.94 |
| A10 | Nil | 174.30 | 74.73 | 0.43 | 174.31 | 75.07 | 0.44 | 146.24 | 321.15 | 1.87 |
| A11 | Nil | 167.08 | 161.14 | 0.91 | 168.07 | 149.78 | 0.84 | 140.20 | 147.29 | 0.83 |
| A12 | Nil | 159.30 | 264.57 | 1.46 | 159.31 | 280.81 | 1.55 | 132.73 | 259.44 | 1.43 |
| A13 | Lawo Ravo | 159.12 | 73.96 | 0.43 | 159.12 | 74.41 | 0.44 | 137.57 | 380.77 | 2.24 |
| A14 | Nil | 128.00 | 343.64 | 1.72 | 127.85 | 344.49 | 1.72 | 106.45 | 343.65 | 1.72 |

The three major discharge values obtained at certain nodes in Table 4 for the 3 used DEMs shows the heights where the inundation will occur in the study area and its environs. The results presented in Figures 5a - 5c shows that when the 30 m and 15 m DEMs were used for the flood modelling, estimated flood heights of 200 m, 250 m and 280 m were capable of flooding the entire floodplain of Shiroro and its environs. In the case of the 3 m UAV derived DEM, significant flood heights of 150 m, 205 m and 250 m, respectively, were estimated and found to be capable of flooding the entire floodplain of Shiroro Dam and its environs.

Similarly, Tables 5 and 6a-b show the number and names of the settlements that would be affected by the various flood levels considering the various DEMs used for the study. The various flood levels were thereafter simulated in the ArcScene environment to create a flood vulnerability graphical model for the study area based on the various identified flood levels (Figures 6a - c).

**(a)**

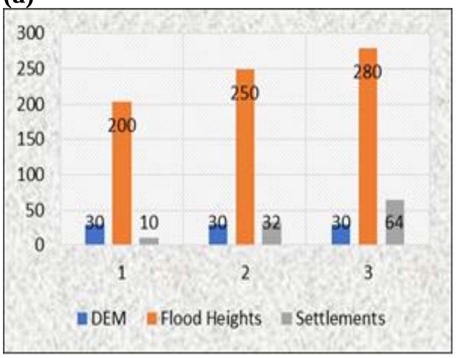


**(b)**

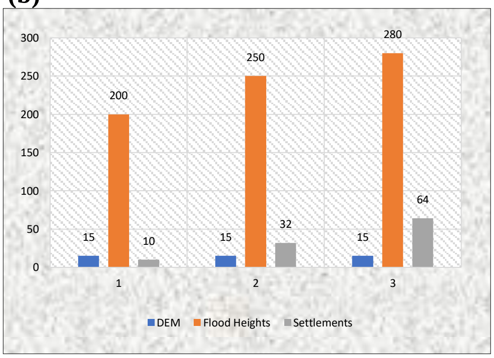

**(c)**

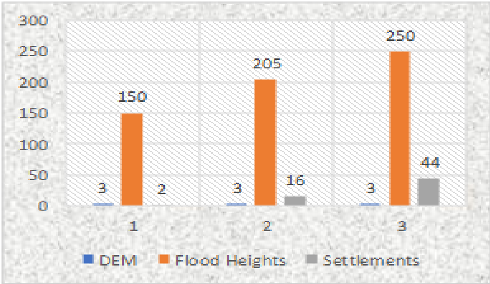


**Figure 5: (a) Flood-heights of 30 m SRTM DEM based on 200m, 250m and 280m (b) Flood-heights of 15 m Resampled SRTM DEM based on 200m, 250m and 280m (c) Flood height of UAV 3 m DEM based 150 m, 205 m and 250 m**

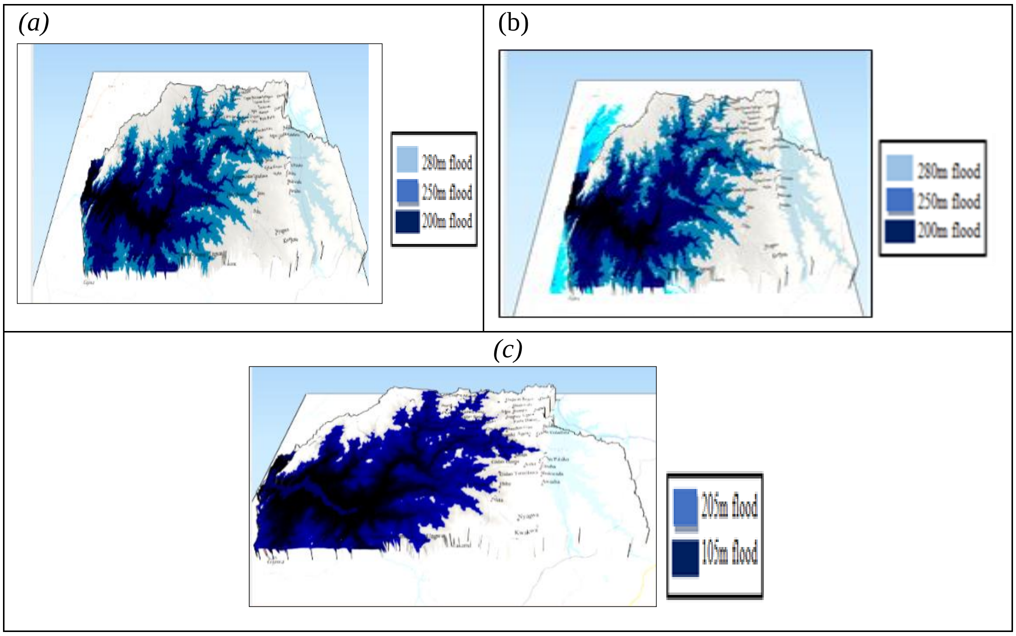


**Figure 6: (a) Vulnerability graphical model for the study area based on 30 m DEM; 200 m, 250 m and 280 m flood extents (b) Vulnerability graphical model for the study area based on 15 m DEM; 200 m, 250 m and 280 m flood extents (c) Vulnerability graphical model for the study area based on 3 m DEM; 150 m, 205 m and 250 m flood extents**

**Table 5: Number of settlements that are vulnerable based on flood levels for the three DEMs**

| 30 m DEM flood levels | | | 15 m DEM flood levels | | | 3 m DEM flood levels | | |
|---|---|---|---|---|---|---|---|---|
| Flood Extents | | | Flood Extents | | | Flood Extents | | |
| 204 m | 250 m | 280 m | 204 m | 250 m | 280 m | 150 m | 205 m | 250 m |
| Vulnerable Settlements | | | Vulnerable Settlements | | | Vulnerable Settlements | | |
| 10 | 32 | 64 | 8 | 28 | 60 | 2 | 16 | 44 |

**Table 6a: Name of settlements vulnerable to inundation at 200 m, 250 m and 280 m flood heights deduced from 30 m and 15 m DEMs**

| Flood Height (200 m) | Flood Height (250 m) | | | | | Flood Height (280 m) | | | |
|---|---|---|---|---|---|---|---|---|---|
| **Settlements Name** | **Settlements Name** | | | | | **Settlements Name** | | | |
| Lawo | Lawo | Gidan Gwari | Gidan | Luwa | Dami | Gidan Gwari | Samboro | Kafa | Gwadaro |
| Manta | Luwa | Maguga | Sumila | Sabon Gida | Gidan Sarumai | GidanUsisi | Manta | Gidan Madatsi | Kawo |
| Maikakaki | Sabon | Maowo | Bere | Gijiwa | Gidan Madaki | Masuku | Kami | Gidan Basakuri | Tungan Makuha |
| Jiko | Gijiwa | Zungoro | Tungan Gamba | Rawo | Gidan Peleta | Gidan Maikomo | Seikna | Padgaya | Guadaguri |
| Kami | Kunu | Rawo | Gini | Kunu | Gidan Saraki | Madaka | Asape Hill | Sumaila | Gwaria |
| Seikna | Kwochi | Manta | Kurmin Gurmana | Kwochi | Kaura Pawa | Kakuri | Guwa | Awolu | Masuku |
| Asape | Kami | Jiko | Gidan Madatsi | Kami | Kwatayi | Tungan Dada | Berikago | Baha | GidanWani |
| Berikago | Layi | Maikakaki | Mangwa | Seikna | Gidan Bako | Gbaro Allah | Tungan Gamba | Gini | Zungoro |
| Zungeru | Seikna | Tunga Dada | Kauran Pawa | Layi | Shamiki | KurminGurmana | Bere | Gusuru | |
| Rafi | Guwa | Samboro | | Jiko | Gwope | Yako | Gijiwa | Yelwa | |
| | Berikago Guwa | Berikaga | | Manta | Magwa | Maowo | GidanMagwi | Maguga | |

**Table 6b: Name of settlements vulnerable to inundation at 150 m, 205 m and 250 m flood heights deduced from 3 m DEM**

| Flood Height (150 m) | Flood Height (205) m | Flood Height (250 m) | | |
|---|---|---|---|---|
| **Settlements Name** | **Settlements Name** | **Settlements Name** | | |
| Jiko | Bere | Kawo | Kauran Pawa | Seikna |
| Maikakaki | Gidan Madaki | Tunga Makubo | Gijiwa | Kami |
| | Sumaila | Gwadara Irina | Maowo | Guwa |
| | Maowo | Gidan Sarumai | Zungoro | Berikago |
| | Tungan Gamba | GidanMadaki | Masuku | Ungwan Zarumayi |
| | Guwa | Dami | Maguga | Kwochi |
| | Berikago | Gwope | Bero | Kunu |
| | Layi | Shamiki | Tunga Gamba | Sabon |
| | Seikna | Yako | Guwa | Luwa |
| | Kami | Gusuru | Berikago | Gijiwi |
| | Gidan Madatsi | Awolu | Kafa | Sabon |
| | Kunu | Baha | Padgaya | Lawo |
| | Luwa | Gini | Gidan Basakri | |
| | Sabon | Yelwa | Gidan Madatsi | |
| | Rawo | Kuemin Gurmana | Sumaila | |
| | Gijiwa | Kwatayi | Layi | |

The identified three flood-risk levels conformed to earlier studies conducted to determine flood risk communities affected by violent water within Niger State, Nigeria (NSEMA, 2021). Although, earlier works by NSEMA (2021) has also identified three flood-risk zones (low, medium and high), it did not identify the flood heights where the risks are high as this study has done. Also, comparing the results obtained in this study with the earlier study of NSEMA (2021), it can be observed that only the 3 m DEM conformed with the existing ground condition (NSEMA, 2021) while the two other DEMs (i.e. the 30m and 15 m SRTM DEMs) over-predicted the flood risk situation.

## CONCLUSION

The performance of 3 DEMs for flood modelling was evaluated in this study with the aid of flood inundation modelling tools in the Arc Scene environment of ArcGIS using the Navier Stokes St. Venant equation. The findings from the study confirmed that accurate terrain data has a great impact on modelling flood hazard. Specifically, the results of flood simulations varied in response to different DEM resolutions, which could be associated with the degree of topography representation of these DEMs. It was also discovered that high-resolution DEM can provide relevant and reliable flood modelling results while in contrast, low resolution DEMs deteriorates the performance of flood models. The UAV-derived flood hazard maps provide more defined flood extent and clearly show the distribution of hazard levels. Hence, a high-resolution DEM is necessary if the decision-maker is interested in local-scale inundation predictions. Further, the use of accurate DEM for flood simulation can provide an initial assessment of the possible population and areas that could be affected by low, medium and high flood hazard. In this study, it was discovered that the realistic flood levels within the Shiroro floodplains were 150 m, 205 m and 250 m as against the 200 m, 250 m and 280 m flood levels obtained from the SRTM data. Such evaluation is useful for determination of possible evacuation centres and establishment of major infrastructure for the populace around the floodplain.

Based on the outcome of the study, it can be concluded that the choice of resampling a low accuracy DEM might not necessarily suffice in improving the modelling capacity of a DEM as it will not significantly improve the quality of the flood modelling. It is concluded that accurate simulation of topography has significant effect on flood simulation results. The study has scientifically justified the reason for the 2012 flood extent got to the affected communities along the Shiroro dam floodplain.

## REFERENCES

Abayomi, K. I., Murtala, A. I., Babatunde, O. & Suleiman, A. (2015). Trend Analysis of Hydro-Meteorological data for river Kaduna at Shiroro Dam Site, Niger State, Nigeria. *Journal of Scientific Research and Reports*, 8(5), 1-12.

Adie, D.B. Ismail, A., Uhammad, M.M & Aliyu, U.B. (2012). Analysis of the Water Resources Potential and Useful Life of the Shiroro Dam, Nigerian. *Journal of Basic and Applied Science*, 20(4), 341-348. http://www.ajol.info/index.php/njbas/index.

Aerts, J.C.J.H., Botzen, W.J.W., Emanuel, K., Lin, N., De Moel, H. & Michel-Kerjan, E.O. (2014). Evaluating Flood Resilience Strategies for Coastal Megacities. *Science*, 344(6183) 473–475.

Anzaku, M. Iliyasu, B.Y., Alfred, O. F., Idoko, A.M. & Sa'adu, S. D. (2019). Evaluation of Environmental Effect of Shiroro Hydropower Dam on the Downstream Communities of Shiroro Local Government Area, Niger State, Nigeria. *Journal of Environment and Earth Science*, DOI: 10.7176/JEES.

Azizian, A. & Brocca, L. (2020). Determining the best remotely sensed DEM for flood inundation mapping in data sparse regions. *International Journal Remote Sensing*, 41, 1884–1906.

https://doi.org/10.1080/01431161.2019.1677968.

Balica, S.F., Wright, N.G. & Van der Meulen, F. (2012). A flood vulnerability Index for Coastal Cities and its Use in Assessing Climate Change Impacts. *Journal of Natural Hazards,* 64(1), 73–105.

Barraga´n, J.M. & De Andre, M. (2015). Analysis and Trends of the World's Coastal Cities and Agglomerations. *Ocean & Coastal Management,* 114, 11–20.

Bhuyian, M. & Kalyanapu, A. (2018). Accounting Digital Elevation Uncertainty for Flood Consequence Assessment. *Journal of Flood Risk Management*, 11(S2), S1051–S1062.

Brunner, G. Savant, G. & Ronald, H. (2020). Modeller Application Guidance for Steady versus Unsteady, and 1D versus 2D versus 3D Hydraulic Modelling. Available at: www.hec.usace.army.mil

Corringham, T.W. & Cayan, D.R. (2019). The Effect of Flood Damages in the Western United States Weather. *Climate Society*, 11, 489–504. https://doi.org/10.1175/ WCAS-D-18-0071.1.

Egbenta, I., Udo, G. & Otegbulu, A. (2015). Using Hedonic Price Model to Estimate Effects of Flood on Real Property Value in Lokoja, Nigeria. *International Journal of Scientific & Engineering Research*, 11(12),

Environment Agency, (2018). Environment Agency - Data [WWW Document]. URL <https://data.gov.uk/search?filters%5Bpublisher%5D=Environment Agency> (accessed 4.1.18). Google Earth Map

Hawker, L., Bates, P., Neal, J. & Rougier, J. (2018). Perspectives on Digital Elevation Model (DEM) Simulation for Flood Modelling in the Absence of a High-Accuracy Open Access Global DEM. Frontiers in Earth Science 6: Article 233.

Jafarzadegan, K., and V. Merwade. (2017). A DEM-Based Approach for Large-Scale Floodplain Mapping in Ungauged Watersheds. *Journal of Hydrology*, 550, 650–662.

Karamuz, E., Romanowicz, R., and Doroszkiewicz, J. (2020). The Use of Unmanned Aerial Vehicles in flood Hazard Assessment. *Journal of Flood Risk Management*, 13(4), Article e12622.

Keshtkar, H., Voigt, W., and Alizadeh, E. (2017). Land-Cover Classification and Analysis of Change Using Machine-Learning Classifiers and Multi-Temporal Remote Sensing Imagery. *Arab Journal Geoscience,* 0(6),154.

Kepengn Xu., Jiayi, F., Yongqiang, F., Qinke, S., Chengbo, W & Min, L. (2021). The Importance of Digital Elevation Model Selection in Flood Simulation and a Proposed Method to Reduce DEM Errors: A Case Study in Shanghai *International Journal Disaster Risk Science,* 12, 890–902 www.ijdrs.com. https://doi.org/10.1007/s13753-021-00377-z

Komolafe, A. A. (2015). A Review of Flood Risk Analysis in Nigeria. *American Journal of Environmental Sciences*, 11, 157-166. https://doi.org/10.3844/ajessp.2015.157.166

Laxmi, B. M. & Narendra, M.S. (2016). Comparative Study of One Dimensional and Two-Dimensional Steady Surface Flow Analysis. *Journal of Advanced College of Engineering and Management*, 2,

Lim, N. & S. Brandt. (2019). Flood Map Boundary Sensitivity Due to Combined Effects of DEM Resolution and Roughness in Relation to Model Performance. Geomatics, Natural Hazards and Risk 10(1): 1613–1647. Ministry of land and survey, Minna, Niger State.

Mohamed, N. & Ali, G. (2019). Investigating Added Value of

Improved DEM, River Geometry, and Model Parameter Definitions on Flood Inundation Mapping. *Proceedings SPIE 11149, Remote Sensing for Agriculture, Ecosystems and Hydrology* XXI, 1114913. doi: 10.1117/12.2532745

Mukherjee, S., Joshi, P.K., Ghosh, A., Garg, R.D. & Mukhopadhyay, A. (2013). Evaluation of Vertical Accuracy of Open Source Digital Elevation Model (DEM). *International Journal of Applied Earth Observation and Geoinformation*, 21(1), 205–217.

Nigeria National Emergency Management Agency (2020)

Nkwunonwo, U.C M. & Whitworth, B. B. (2019). Urban flood Modelling Combining Cellular Automata

Framework with Semi-Implicit Finite Difference Numerical Formulation. *Journal of Africa Earth Science* 150, 272–281.

Niger State Emergency Management Agency (2021). Studies Conducted to Determine Flood Risk Communities Affected by Violent Water within Niger State, Nigeria

Ogania, J.L., Puno, G.R., Alivio, M.B.T. & Taylaran, J.M.G. (2019). Effect of digital elevation model's resolution in producing flood hazard maps. *Global Journal Environmental Science Management*, 5, 95–106. https://doi.org/10.22034/gjesm.2019.01.08.

Ozdemir, H., Sampson, C.C., de Almeida, G.A.M. & Bates, P.D. (2013). Evaluating scale and Roughness Effects in urban flood modelling using terrestrial LIDAR data. *Hydrology Earth System Science*, 17, 4015–4030. https://doi.org/10.5194/hess-17-4015-2013.

Pena, F. & Nardi, F. (2018). Floodplain Terrain Analysis for Coarse Resolution 2D flood Modelling. *Journal of Hydrology,* 5. https://doi.org/10.3390/hydrology5040052.

Pottier, N., Penning-Roswell, E., Tunstall, S. & Hubert, G. (2005). Land Use and Flood Protection: Contrasting Approaches and Outcomes in France and in England and Wales. *Journal of Applied Geography*, 25, 1–27. https://doi.org/10.1016/j.apgeog.2004.11.003

Saksena, S. & Merwade, V. (2015). Incorporating the Effect of DEM Resolution and Accuracy for Improved flood Inundation Mapping. *Journal of Hydrology*, 530, 180–194. https://doi.org/ 10.1016/j.jhydrol.2015.09.069.

Suleiman, Y.M. (2014). The Role of Rainfall Variability in Reservoir Storage Management at Shiroro Hydropower Dam, Nigeria. *An International Journal of Science and Technology*, 3(2), http://dx.doi.org/10.4314/stech.v3i2.2

Talchabhadel, R., Nakagawa, H., Kawaike, K. Yamanoi, K. & Thapa, B.R. (2021). Assessment of Vertical Accuracy of Open source 30m Resolution Space-Borne Digital Elevation Models. *Geomatics, Natural Hazards and Risk*, 12(1), 939–960.

Tarekegn, T., Haile, A., Rientjes, T., Reggiani, P. & Alkema, D. (2010). Assessment of an ASTER-Generated DEM for 2D Hydrodynamic Flood Modelling. *International Journal of Applied Earth Observation and Geoinformatics*, 12(6), 457-465.

Usman, A. & Ifabiyi, I. (2012). Socio-Economic Analysis of the Operational Impacts of Shiroro Hydropower Generation in the Lowland. *International Journal of Academic Research in Business and Social Sciences*, 2(4)

Ward, P.J., Jongman, B., Kummu, M., Dettinger, M.D., Sperna Weiland, F.C. & Winsemius, H.C. (2014). Strong Influence of Southern Oscillation on Flood Risk around the World. *Proceedings of National*

*Academic Science* U. S. A. 111, 15659–15664. https://doi. org/10.1073/pnas.1409822111.topic s/floods#tab=tab_2> (accessed 4.29.20).

World Health Organisation (2020). Flood [WWW Document]. URL <https://www. who.int/health

Zazo, S., Molina, J.L. & Rodríguez-González, P. (2015). Analysis of Flood Modelling through Innovative Geomatic Methods. *Journal of Hydrology*, 524, 522-537.